JPRS-JST-92-033
22 DECEMBER 1992

JPRS Report

Science & Technology

Japan

CERAMICS SOCIETY OF JAPAN
1992 MEETING

JPRS-JST-92-033
22 DECEMBER 1992

SCIENCE & TECHNOLOGY
JAPAN

CERAMICS SOCIETY OF JAPAN 1992 MEETING

926C0095 Tokyo NIPPON SERAMIKKUSU KYOKAI 1992 NENKAI KOEN YOKOSHU in Japanese
20 May 92 pp 1-555

[Selected papers from the 1992 Annual Meeting of the Ceramics Society of Japan held 20-22 May 92 in Tokyo and sponsored by the Ceramics Society of Japan]

CONTENTS

Preparation of $SrTiO_3$-Based High Dielectric Films by Sol-Gel Processing

926C0095A Tokyo NIPPON SERAMIKKUSU KYOKAI 1992 NENKAI KOEN YOKOSHU in Japanese 20 May 92 p 4

[Article by Hiroyuki Nishimura, Hiroshi Adachi, and Hirozo Kanegae, Biology Laboratory, Mitsubishi Electric Corp.]

[Text] **Abstract:** $SrTiO_3$(ST) and $SrTiO_3$–Bi_2O_3–TiO_2(SBT) thin films were synthesized as follows: 1) spin coating the uniform and stable isopropanol solution of mixed alkoxides with acetylacetone as stabilizer on the plutonium substrate, and 2) firing at 700°C under O_2. The film thicknesses and dielectric constant were 2100 Å and 270 for ST, 2700 Å and 511 for SBT, respectively.

Introduction

As high dielectric thin film materials, PZT and PLZT have been actively studied but they are ferro-dielectric substances having piezoelectric properties, and their long-term reliabilities are suspect due to their mechanical distortions. In this study, we took note of $SrTiO_3$-based thin films as a constant dielectric high-dielectric substance and examined them using the sol-gel processing which allows manufacturing a uniform thin film at comparatively inexpensive cost. Following is a report on its preparation method.

Experiment Method

A flow chart of the thin film preparation is shown in Figure 1. The raw material alkoxides were mixed so that $Sr(OiPr)_2/Ti(OiPr)_4$ becomes 1/1 (mol ratio %) in SrTiO3(ST) thin films and $SrTiO_3/Bi_2O_3/TiO_2$ becomes 75/15/10 (wt%) in $SrTiO_3$–Bi_2O_3–TiO_2(SBT) thin films. As a stabilizer, acetylacetone was added to acquire a coating solution through hydrolysis. As a substrate, we used a thermal-oxide film-coated silicon wafer with Pt film growth as the lower electrode.

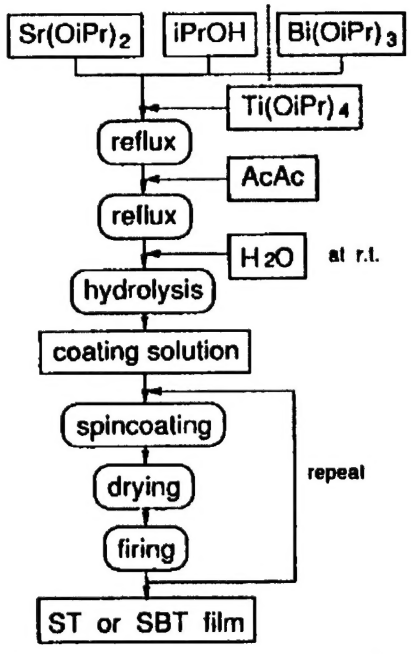

Figure 1. Flow Diagram for Processing of $SrTiO_3$ and $SrTiO_3$–Bi_2O_3–TiO_2 Films

For filming, a spin coating processing was used and, after being dried at room temperature and 150°C, calcined tentatively at 620°C. To raise the film thicknesses, this processing was repeated several times and finally it was calcined for one hour at 700°C to acquire ST and SBT thin films. The drying and calcination were all done under oxygen atmosphere. The crystal structures of the acquired thin films were identified by X-ray diffraction (XRD) and their film thicknesses were measured and their cross sections were observed using scanning electron microscope (SEM). Their electrical properties were measured with the Pt film coated on the thin film as the upper electrode: dielectric constant and dielectric loss by an LCR meter and leak current by a picoammeter.

Experimental Results

The raw material alkoxide are all unstable substances, but we could acquire a stable light-yellow transparent sol solution even after hydrolysis by virtue of the acetylacetone for stabilization. For ST, coatings were repeated six times to acquire a film thickness of 2100 Å and for SBT, five times for a thickness of 2700 Å. The dielectric constants were 270 and 511 each and the leak currents were 9.0×10^{-9} and 2.4×10^{-8}A/cm^2 at 1.65 V, respectively. When the calcination was done under atmosphere, the leak current became more than 10^{-5}, suggesting that oxygen greatly contributes to the leak current drop. From the XRD result, it was found that both films have a strong (111) orientation.

Preparation, Dielectric Properties of $Bi_4Ti_3O_{12}$ Thin Films by Sol-Gel Process

926C0095B Tokyo NIPPON SERAMIKKUSU KYOKAI 1992 NENKAI KOEN YOKOSHU in Japanese 20 May 92 p 11

[Article by Noboru Toge, Yoshifumi Fukuda, and Tsutomu Minami, University of Osaka Prefecture]

[Text] **Abstract:** $Bi_4Ti_3O_{12}$ thin films were prepared from corresponding metal alkoxides stabilized with amines and acetylacetones. The optimization of the preparation conditions produced the films of the $Bi_4Ti_3O_{12}$ single phase after the heat treatment over 500°C. These films have the dielectric constant of 124 and the loss of 0.04 at 10 kHz.

Introduction

The chemical compound $Bi_4Ti_3O_{12}$ (BIT) has a layered structure of the $[Bi_2O_2]^{2+}$ layer and $[Bi_4Ti_3O_{10}]^{2-}$ perovskite phase and it is expected to be applied to Pb-free systems such as ferroelectric memory. The thin filming process of these ferroelectric substances are tested mainly in the gaseous phase process. In this study, we prepared thin films by the sol-gel process and examined their properties.

Experiment

As the starting raw materials, an ethanol solution of $Bi(OEt)_3$ (manufactured by Hakusui Chemicals) and $Ti(O\text{-}n\text{-}Bu)_4$ were used after stabilizing them with acetylacetone. They were mixed with a ratio of Bi:Ti = 4:3 and made into a coating solution through hydrolysis. Then, it was coated on a quartz glass of Pt substance in the atmosphere and heat treated at 400°C. After repeating this coating and heat treatment, Ti was further heat treated at a high temperature and a thin film of about 1 μm thickness was acquired.

Result

Depending on conditions of preparing thin films, Bi_2O_3 in addition to BIT was precipitated. The BIT single-phase film was acquired by making the concentration of coating solution rather low and expediting the hydrolysis and condensation/polarization of alkoxides. These thin films were transparent above the wavelength of 340 nm in contrast to the yellowish opaque precipitation of Bi_2O_3.

Figure 1 shows the X-ray diffraction patterns of thin films (Pt substrate) heat treated at various temperatures. Though they are almost amorphous at 400°C, a pseudo tetragonal BIT was precipitated above 500°C. As the treatment temperature rises, the BIT crystallinity was upgraded and neared a diffraction pattern of the powder acquired from the coating solution. No orientation was observed in particular for these thin films.

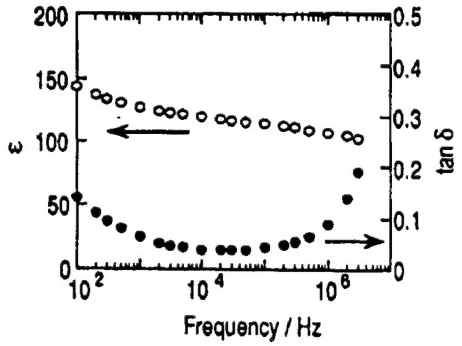

Figure 2. Dielectric Properties of BIT Films Heat-Treated at 500°C

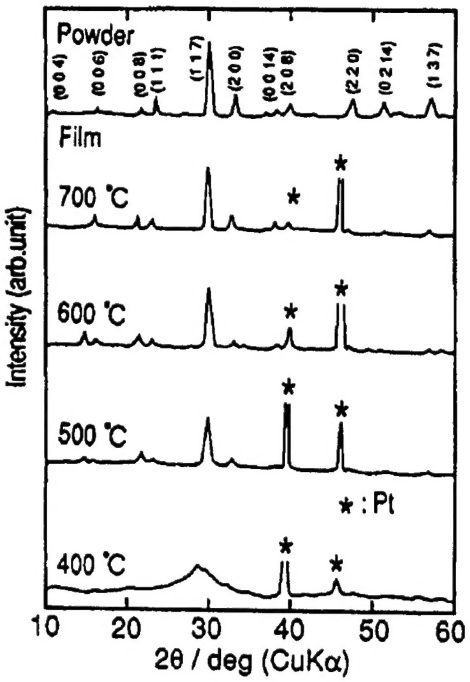

Figure 1. X-Ray Diffraction Patterns of BIT Films Heat-Treated at Different Temperatures

Figure 2 shows the dielectric properties of thin films heat treated at 500°C. The dielectric constant at 10 kHz was 124 and dielectric loss was 0.04, comparable to the properties acquired through the solid phase method.

These results indicate that it is possible to prepare layered BIT dielectric thin films at comparatively low temperature by the sol-gel process.

Synthesis of Perovskite $Pb(Ni_{1/3}Nb_{2/3})O_3$ by Sol-Gel Process

926C0095C Tokyo NIPPON SERAMIKKUSU KYOKAI 1992 NENKAI KOEN YOKOSHU in Japanese 20 May 92 p 12

[Article by Seiji Takahashi, Satoru Yoneda, and Makoto Kuwabara, Kyushu Institute of Technology]

[Text] **Abstract**: Power of $Pb(Ni_{1/3}Nb_{2/3})O_3$ (PNN) was prepared by the sol-gel method. The powder calcined at 800°C for two hours was composed of a columbite, $NiNb_2O_6$ and a pyrochlore, $Pb_2Nb_2O_7$. It was considered that each component which was mixed homogeneously in solution was segregated during hydrolysis and condensation.

The perovskite phase was synthesized by calcination at higher than 850°C.

The dielectric ϵ_r of composite perovskite $Pb(Ni_{1/3}Nb_{2/3})O_3$ (hereinafter PNN) near the Curie point is about 4,000 and at room temperature about 1,500. In addition to this feature, the Curie point can be varied over a wide range by solid solution with other components due to its Tc = -120°C and it is regarded as a promising capacitor material with high dielectric constant. In this study, we compared the preparation results obtained from the solid phase method and sol-gel method, aiming at synthesizing the PNN at low-temperature through the sol-gel process.

As the starting materials, PbO and $NiNb_2O_6$ were used for the solid phase process and $Pb(OAc)_2$, $Ni(acac)_2$, and $Nb(OEt)_5$ for the sol-gel process. In the sol-gel process, methoxyethanol was used as a solvent and the experiment was carried out in a nitrogen atmosphere. To identify the phase, the powder X-ray diffraction method (XRD) was used.

In the solid phase method, a columbite and pyrochlore phase which did not react at 800°C was observed. It is presumed that nonreactive Nb_2O_5 remains in the columbite and it reacts with PbO generating the pyrochlore phase. At 850°C, perovskite phase of a few percent was observed in the pyrochlore phase. On the other hand, at 900°C pyrochlore phase of a few percent was observed in the perovskite phase.

When the acquired sol solution was dripped into an excessive amount of water to make a gel form by force in the sol-gel method, only a pyrochlore phase was

observed at 800°C and massive pyrochlore phases simultaneously mixed with a perovskite phase were observed at 850°C and 900°C.

Figure 1 shows an XRD chart of the calcined powder acquired by the gel processing when a sol solution is added with 50 mol times more water ad kept at 90°C for drying. At 800°C, the coexistence of pyrochlore and columbine phases was observed and almost the same result as that of the solid phase method was realized at 850°C and 900°C. In the preparation process of the sol-gel method carried out this time, the reason the calcination conditions generating the perovskite are almost the same as those of the solid-phase method is presumed to be that the organic metallic compounds (PNN precursor) including several metals required in the PNN sol solution in its preparation are not formed and gel processing progresses nonuniformly through hydrolysis. We are now studying sol-gel processes and hydrolysis conditions so that a satisfactory PNN precursor can be acquired.

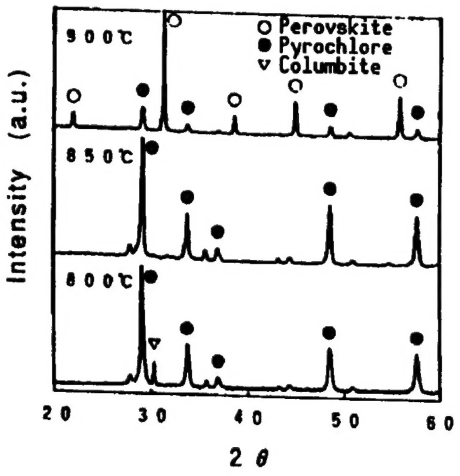

Figure 1. XRD Chart
(Gel powder kept stationary at 90°C)

High-Resolution Electron Microscopy of Hot-Pressed Si_3N_4-SiC Nanocomposite Materials

926C0095D Tokyo NIPPON SERAMIKKUSU KYOKAI 1992 NENKAI KOEN YOKOSHU in Japanese 20 May 92 p 83

[Article by Gen Sasaki, Katsuaki Suganuma, and Teruaki Fujita, National Self-Defense Agency; Kenji Hiraga, Tohoku University; and Koichi Niihara, Osaka University]

[Text] **Abstract**: Si_3N_4-SiC nanocomposite was fabricated by hot pressing the mixture of SiC and Si_3N_4 fine powders. SiC particles showed two distributions as follows: dispersing uniformly in Si_3N_4 grains and condensing at grain boundaries of Si_3N_4. The interface between SiC and Si_3N_4 in case of the former distribution showed the disturbed structure having less than 1 nm in thickness and had a tendency to be flat along $(111)_{SiC}$ plane.

Introduction

We reported earlier that the Si_3N_4/SiC nanocomposite material having excellent mechanical properties could be manufactured by mixing and hot pressing SiC and Si_3N_4 micropowders, but its microstructure has not been clarified yet. In composite materials in particular, the interface of different phases is an important factor to determine their mechanical properties. Therefore, we aimed at analyzing their microstructures at a level of atoms centering on the Si_3N_4/SiC interface using a high-resolution transmission electron microscope.

Experimental Method

The α-Si_3N_4 powder of average grain size of 0.2 μm (SNE-10 manufactured by Ube Kosan Industries) was mixed (10 vol%) with the β-SiC powder of average grain size of 0.3 μm (Ultra-Fine manufactured by Ibiden Inc.) and the 8 wt% Y_2O_3 was added to aid sintering (manufactured by Nippon Yttrium Engineering). Then, after a wet ball mill mixture with ethanol, the hot-pressed sintering was conducted to acquire the specimen. The sintering conditions were in an N2 atmosphere with a pressure of 30 MPa, temperature of 2,073 K, time of 60 minutes. The specimen was fabricated to a thickness of 40 μm, thin filmed for electron microscope observation by means of ion thinning. The transmission electron microscopes (TEM) used were JEM-200CX and 4000EX from Nippon Electronic Inc.

Results

There were two patterns in SiC particles distributed in β-Si_3N_4 grains with sizes of several dozen nm and coagulated at the grain boundaries. The interface of SiC and Si_3N_4 distributed in grains had a disturbed structure with a thickness less than 1 nm (Figure 1). The SiC particles had a tendency to form a flat interface along the (111) plane. The β-Si_3N_4 particles grown like pillars grew along the (100) plane and this plane often became the grain boundary. The interface between those β-Si_3N_4 particles was observed with a grain boundary phase and without it.

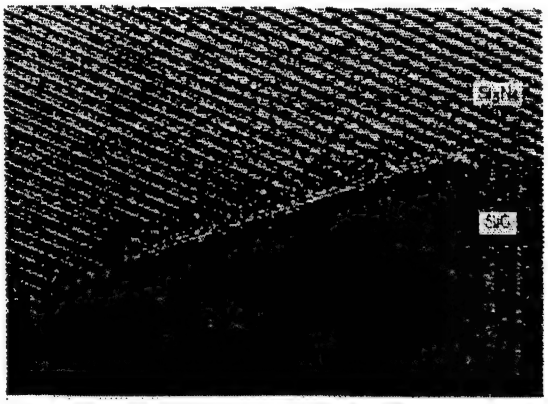

Figure 1. High Resolution Observation of Interface Between SiC and Si_3N_4

High-Pressure Hot Pressing of TiC Using SHS Reaction

926C0095E Tokyo NIPPON SERAMIKKUSU KYOKAI 1992 NENKAI KOEN YOKOSHU in Japanese 20 May 92 p 84

[Article by Toshihiko Nishida and Naoko Miyazaki, Kyoto Institute of Technology, and Kazunori Urabe, Ryukoku University]

[Text] **Abstract:** High pressure (10,000 atm) was applied to the powder mixture of Ti and C during self-propagating reaction. Vickers hardness of the obtained polycrystalline TiC and TiC with 10 wt% Al_2O_3 was 19 and 27 GPa, respectively.

Introduction

The self-propagating high-temperature synthesis (SHS) method has attracted attention as one of the new synthesis methods for inorganic compounds having high melting points. This hot-pressing process allows a simultaneous synthesis and sintering of ceramics with a self-propagating heating reaction in synthesis, featuring use of the reaction heat not the external heating in the driving force of sintering. In this study, we aimed at synthesizing TiC and TiC-based composite materials using this self-propagating heating reaction and promoting the densification of hard-to-sinter ceramics by applying high pressure for a short time during the self-propagating heating.

Experimental Method

High-purity fine particle raw materials of metallic titanium and graphite were wet blended and an oxide raw material was added in a proper wet blending. The acquired blended powder of about 60 grams was dried and shifted to a pressure-proof double-sintered mold (inner diameter of 35 mm) having simplified graphite sheet insulation, and fabricated tentatively with a pressure of 49 MPa. Then, the compact was ignited by attaching a tungsten heater to its edge to start the self-propagating reaction and, by applying a high pressure of 980 MPa (10,000 atm) during the reaction, a short-time single-axis hot pressing was carried out. The acquired sintered body was analyzed for X-ray diffraction, Vickers hardness and its structure was observed using a scanning electron microscope (SEM) and transmission electron microscope (TEM).

Results

A part of the results is shown in Table 1. When Ti was blended with C with an equal mol ratio, a dense sintered body of TiC single phase was observed through X-ray diffraction analysis and its average hardness (HV) was 18.7 GPa. However, when the blending was done without an equal mol percentage, the self-propagating heating reaction became unstable and stopped when pressure was applied, with a lowering of the density of acquired sintered body.

Table 1. Composition and Some Properties of SHS/HP Specimens

No.	Ti	C	M mol%	HV GPa	X-ray	Color
1	50	50	0	18.7	TiC	Gray
2	55	45	0	10.7	TiC	Gray
3	60	40	0	–	TiC	Gray
4	48.4	48.4	Al_2O_3 3.2	27.0	TiC	Gray
5	48.7	48.7	ZrO_2 2.6	–	TiC	Gray
6	45	45	0		x	
7	46.2	46.2	MgO 7.6		x	

Further, an experiment when 10 wt% of the oxide powder was added to a mixture of Ti and C of equal mol ratio, a second phase having much Al contents was generated at the grain boundary when alumina was added, and it was confirmed that the TiC particle growth was constrained in the acquired sintered body and the hardness (HV) was improved to 27.0 GPa. From these experimental results, it was known that it is possible to manufacture a high-density sintered body during the self-propagating heating reaction of Ti-C materials just by applying a short-time pressure. However, it is necessary to upgrade the programs for the ignition method and pressurization as some acquired sintered bodies tend to generate air gaps and cause a delamination in the direction vertical to the pressure-applying axis.

Reinforcing Al_2O_3/TiC Nanocomposites by ZrO_2

926C0095F Tokyo NIPPON SERAMIKKUSU KYOKAI 1992 NENKAI KOEN YOKOSHU in Japanese 20 May 92 p 171

[Article by Ryuichi Matsuki, Hisao Ueda, and Takeyoshi Takenouchi, Mitsubishi Materials Co., Ltd., and Atsushi Nakahira and Koichi Niihara, ISIR, Osaka University]

[Text] **Abstract**: Effects of TiC and ZrO_2 dispersions on the fracture toughness, strength and hardness were investigated for Al_2O_3/TiC/ZrO_2 composites. The Al_2O_3/TiC/ZrO_2 composites were prepared by common hot-pressing the mixture of fine Al_2O_3. TiC and ZrO_2 powders. The fracture toughness and strength of these composites were enhanced by incorporating the TiC and ZrO_2 particles into Al_2O_3 matrix. The strengthening and toughening mechanisms of Al_2O_3/TiC/ZrO_2 composites were discussed.

1. Purpose

We reported last time that the nanocomposite synthesis is effective even with Al_2O_3/TiC materials which have distributed fine TiC particles as the second phase in Al_2O_3 matrix. However, the toughness of this composition was not improved enough even though the strength at room and high temperature was upgraded considerably with the second phase addition by 5 vol%—comparable to that of conventional Al_2O_3/20~30 vol% TiC composite materials. Therefore, we aimed at upgrading the toughness of Al_2O_3/TiC nanocomposites through preparing Al_2O_3/TiC nanocomposites by adding ZrO_2 with different Y_2O_3 volumes and examined its microstructure and mechanical properties.

2. Experimental Method

As the starting raw materials, α-Al_2O_3 (average particle size of 0.4 μm), TiC powder (average particle size of 0.2 μm) and three ZrO_2 types with different Y_2O_3 volumes were used. First, by adding 5 vol% TiC to Al_2O_3 and further adding the specified quantity of either of the three ZrO_2 types, it was blended in a wet ball mill for 24 hours. After heating and drying, it was mixed and crushed in a dry ball mill for 24 hours to acquire a blended powder. This blended powder was hot pressed under the conditions of Ar atmosphere, pressure of 30 MPa and 1,400~1,600°C. The acquired sintered body was cut into rectangular sizes, ground and polished for evaluating various properties and observing

their microstructure. The monoclinic ZrO_2 quantity was determined by the tetragonal (101), monoclinic (111), and the peak height proportion of (111).

3. Experimental Results

For the density of Al_2O_3/5 vol% TiC nanocomposites, the hot-pressing temperature of 1,600°C was required. But in our study of composite materials, the temperature for densification depended strongly on the amount of addition but not on the amount of the Y_2O_3 even though many kinds of ZrO_2 were used.

A dense sintered body was acquired by hot pressing when the ZrO_2 addition was 5~10 vol% at 1,500°C and 20~30 vol% at 1,400°C and the sintering temperature was dropped by 100~200°C by adding ZrO_2.The fracture strength of $Al_2O_3/TiC/ZrO_2$ composite materials with unstable ZrO_2 added is shown in Figure 1. The fracture strength of Al_2O_3/5 vol% TiC nanocomposite 1050 MPa for a sintered body at 1,600°C and the composite material satisfactorily reinforced in our study showed a high strength of more than 1200 MPa.

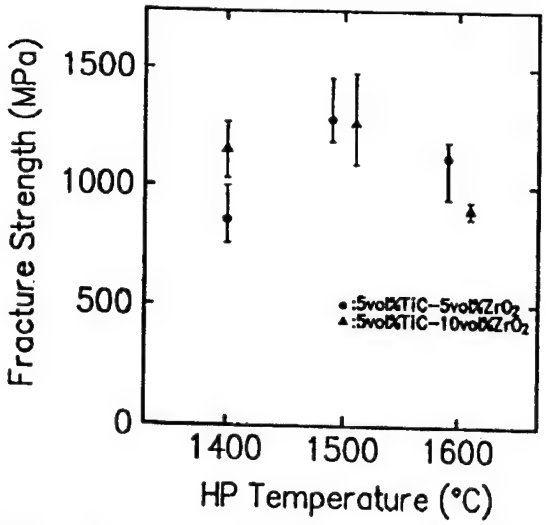

Figure 1. Fracture Strength of $Al_2O_3/TiC/m-ZrO_3$ Composite Material

Observation of Microstructure, Dislocation of Al_2O_3/SiC Nanocomposites

926C0095G Tokyo NIPPON SERAMIKKUSU KYOKAI 1992 NENKAI KOEN YOKOSHU in Japanese 20 May 92 p 172

[Article by Atsushi Nakahira and Koichi Niihara, ISIR, Osaka University, and Yuichi Ikuhara, JFCC]

[Text] **Abstract:** Al_2O_3/SiC nanocomposites were fabricated by hot pressing the mixed powders of ultrafine Al_2O_3 and SiC. The microstructure of Al_2O_3/SiC nanocomposites were investigated by transmission electron microscope (TEM). TEM observation of these nanocomposites showed SiC particles less than 200 nm were uniformly dispersed within the Al_2O_3 matrix grain and dislocation network were seen within Al_2O_3 matrix grains. The relationship of the dislocation and intragranular SiC particle will be discussed in detail for Al_2O_3/SiC nanocomposites.

1. Introduction

It has been known that the mechanical properties of ceramic nanocomposites with the second phase dispersed minutely and uniformly in the intragranular matrix at a nanometer level are drastically superior to those of conventional microcomposite materials. The Al_2O_3/SiC nanocomposites in particular that can be manufactured through hot pressing as in the powder metallurgy achieved a noticeable improvement in their characteristics—high strength of more than 1 GPa in addition to a reinforced toughness by adding SiC. This kind of upgraded mechanical properties are said to be attributable to the minute control of the structure dispersed in SiC and Al_2O_3 particles at a nanolevel but some role splayed by the SiC particle for the intragranular structure control such as the dislocation network, subgrain boundary, residue stress observed in the Al_2O_3 grains are not to be discovered.

In particular, it is vital to clarify the role the dislocation plays for the mechanical properties for designing materials and, furthermore, the relationship between the residue stress and dislocation closely related to the mechanical properties of nanocomposites in our study must be clarified. This study aims at observing the microstructure of Al_2O_3/SiC composites and identifying the dislocation in the Al_2O_3 grains.

2. Experimental Method

The powders used in this experiment were γ-Al_2O_3 (made by Asahi Chemicals) and β-SiC (Ibiden, Inc.). The SiC weighed in at 5~33 vol% using the Al_2O_3 as the matrix. The mixture was blended in a polyethylene container in the wet blending of ethanol using the Al_2O_3 ball for 12 hours, then dried sufficiently and dry blended further for 24 hours. The acquired Al_2O_3/SiC mixture powder was sintered by the hot-pressing process in nitrogen atmosphere. The hot-pressing conditions were under a pressure of 30 MPa at a temperature range of 1,500~2,000°C. The hot-pressed specimen was cut into thin slices which were ion-thinned with Ar ion for TEM observation using a JEOL-CX200.

Figure 1. Transmission Electron Micrograph for Al_2O_3/SiC Nanocomposites

3. Results

Figure 1 shows a TEM micrograph of typical Al_2O_3 nanocomposites. The SiC particles in Al_2O_3 grains were distributed uniformly without coagulation. Furthermore, as seen from the micrograph, the dislocation or network observed in Al_2O_3 grains had a pinning by the SiC particles.

Sintering Mechanism, Nanostructure Control of Al_2O_3 Particulate Powders

926C0095H Tokyo NIPPON SERAMIKKUSU KYOKAI 1992 NENKAI KOEN YOKOSHU in Japanese 20 May 92 p 173

[Article by Masahiro Inoue, Atsushi Nakahira, and Koichi Niihara, ISIR, Osaka University]

[Text] **Abstract:** The sintering behaviors of ultrafine Al_2O_3 powder and Al_2O_3/ 5 vol% SiC powder mixture were studied by scanning electron microscope (SEM) and transmission electron microscope (TEM). The grain coalescence was observed in the initial sintering stage of ultrafine Al_2O_3 by TEM. In the later stage, the grains of Al_2O_3 were confirmed to grow by grain boundary migration. For the Al_2O_3/SiC powder mixture, the nanostructure was found to form by the matrix grain coalescence and the grain boundary migration mechanisms. It is suggested that the structural control of ceramics in nanometer-scale can be effectively performed using the peculiar sintering mechanisms of the ultrafine particles.

1. Introduction

The nanocomposites are new-type composite materials compounding the nano-level minute second phase in crystalline grains or at grain boundaries. These composite materials are designed to control (nanostructure control) in crystal grains at nanolevel by forming micro residue stress fields or subgrain boundaries around the second phase particulates dispersed in the matrix grains (Figure 1). In this report, the relationship between the nanostructure control and sintering mechanism will be discussed.

Figure 1. TEM Micrograph of Al_2O_3/SiC Nanocomposites

2. Experimental Method

As the starting raw materials, particulate powders of γ-Al_2O_3 (manufactured by Ashai Chemicals, average grain size of less than 0.4 μm and primary grain size of about 10 nm) and β-SiC (manufacture by Ibiden Inc., average grain size of less than 0.3 μm) were used. The Al_2O_3 particulates and blended powder of Al_2O_3/ 5 vol% SiC were hot pressed for sintering under the conditions of

1,000~1,600°C, pressure of 30 MPa, holding time of 0 minutes (suspending heating after reaching a specified temperature and cooling the furnace), and changes of their microstructure were observed through microscopy. Further, a status analysis was carried out with X-ray photoelectronic spectroscopy (XPS) in order to examine the nanostructure starting from the atom level.

3. Experimental Results

From the results observed through microscopy, it was suggested that the particulate synthesis process occurred at the early stage of sintering of the Al_2O_3 particulates. Further, it is known that the particle growth occurs as the sintering progresses by shifting the grain boundary around the synthesized particles formed at the early stage. It is presumed that the microstructure can be effectively controlled at a nanometer-level by using a sintering mechanism intrinsic to these particulates.

Manufacturing AlN/Metal Composites by Nitriding Molten Al

926C0095I Tokyo NIPPON SERAMIKKUSU KYOKAI 1992 NENKAI KOEN YOKOSHU in Japanese 20 May 92 p 180

[Article by Keita Inoue, Takanori Watari, Toki Torikai, and Osaku Matsuda, Saga University]

[Text] **Abstract**: AlN/Al composites were prepared by the nitridation of molten Al containing MgO at reaction temperatures from 1,250~1,400°C. The composites consisted of the porous layer and the dense AlN/Al layer. As the content of MgO, the nitridation temperature and the time increased, the thickness of the dense AlN/Al layer increased. Most of the Al metal was converted into AlN at 1,300°C for 2 hours. In this case, the needle-like AlN crystals were observed in the nitrided dense layer.

1. Purpose

It is possible to acquire materials possessing both high toughness, hardness, and strength by compounding ceramics and metals. In our study, we prepared an AlN/Al composite by nitriding molten Al directly at high temperature and examined its compound.

2. Experiment

The MgO powder was blended to the Al powder by 0~10 wt% to form a fabrication with two axes. It was put on an alumina boat and reacted for one-half to three hours at 1,100~1,400°C in nitrogen atmosphere in a circulating longitudinal electric furnace. For comparison, the Mg blending and MgO coating methods were examined as well. The weight increase before and after the reaction was measured and the qualitative analysis and structure observation of the specimen after the reaction as well as the film thickness measurement of nitrided layer were carried out.

3. Results and Analysis

The specimen of Al powder alone was hardly nitrided with a reaction at 1,400°C for one hour and the nitridation rates were about 10 and 20 percent for specimens coated with MgO (5 wt%) and added with Mg (5 wt%), respectively.

However, when MgO was added to the Al powder, the nitridation was facilitated and the nitridation rate rose as the addition of MgO was increased to about 50 percent with an addition of 5 wt%. This specimen consisted of two layers—porous section (upper) and dense one (lower) but both sections were composed of AlN and Al based on a qualitative analysis by X-ray diffraction (XRD). As a result of the structure observation, it was known that the porous section is a remnant of the Al raw material powder and the dense section was an AlN/Al composite formed by continuous nitridation of Al. Generally, in a nitridation of Al metal only, by the surface nitriding film, the subsequent nitridation is restricted. However, it is presumed that MgO broke down the surface film with a certain reaction and expedited the nitridation continuously in our experiment.

Figure 1 shows a time change of the dense layer. The film thickness of fabricated layer increased as the nitridation time was extended to about 2 mm in two hours. The nitridation rate of this specimen reached almost 100 per-cent and the XRD showed the peak of AlN only and needle-like AlN crystals were observed in the structure observation.

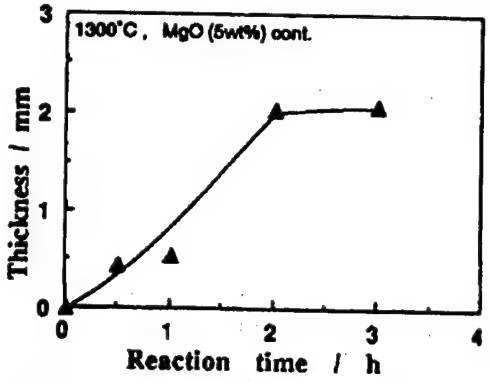

Figure 1. Effect of Reaction Time on Thickness of Dense Products

Preparing SiC/C Functional Gradient Carbon Materials, Their Oxidation

926C0095J Tokyo NIPPON SERAMIKKUSU KYOKAI 1992 NENKAI KOEN YOKOSHU in Japanese 20 May 92 p 333

[Article by Osamu Yamamoto, Keita Imai, and Tadashi Sasamoto, Kanagawa Institute of Technology]

[Text] **Abstract:** SiC/C functionally gradient carbon materials (SiC/C materials) were prepared by silicon impregnation process. The SiC compositionally gradient in the SiC/C materials obtained was possible by controlling reaction temperatures and times. A heat treatment at 1,450°C for three hours in argon resulted in the formation of 100 percent of SiC on the surface of the SiC/C materials. The SiC/C materials showed a high oxidation resistance at 600°C and 1,400°C.

1. Purpose

Carbon materials as the high-temperature structural material have quite excellent properties such as high-temperature stability and high thermal impact resistance but have a disadvantage in that they are oxidized in high-temperature oxide atmosphere and their excellent properties are damaged. As one means to solve this problem, it is conceivable to add an SiC/C gradient function to the carbon materials. The features of this processing hamper oxidation of the carbon by means of the surface SiC and alleviate somewhat quickly the interface separation due to a difference in the thermal expansion coefficients between SiC and carbon materials. In this study, the SiC gradient function was added to the carbon material itself by the silicon impregnation method, and the composition gradient degree and oxidation resistance of the acquired gradient functional carbon materials were discussed.

2. Experiment

The mirror-polished artificial graphite and glass carbon matrix was buried into the silicon powder in a graphite crucible and heated at a specified temperature and for specified hours in argon to create a SiC/C functionally gradient matrix. After polishing the surface of the acquired SiC/C functionally gradient carbon matrix, its composition gradient degree was examined through X-ray diffraction measurement. The oxidation resistance test was carried out under an air flow of 50 ml/minute at a specified temperature.

Further, the surface and cross section of the carbon base material was observed with a scanning electron microscope.

3. Results and Analysis

As a result of examining the composition gradient of artificial graphite and glass carbon material impregnated with silicon, it was discovered that the SiC generation rate on the surface of the artificial graphite as shown in Figure 1 increased as the silicon impregnation temperature and time are extended, to reach a 100 percent generation of SiC at 1,450°C in three hours.

Meanwhile, in a case of the glass carbon base material, the SiC generation rate on the base material surface was about 17 percent. It is presumed this is due to a lower reaction active spot of the glass carbon than that of the black lead. As a result of testing the SiC/C gradient function base material for its oxidation resistance which was acquired after heat treating an artificial graphite base material at 1,450°C for three hours, the oxidation of carbon base material was restricted by about five times at 600°C and about eight times at 1,400°C in comparison with the artificial graphite base material.

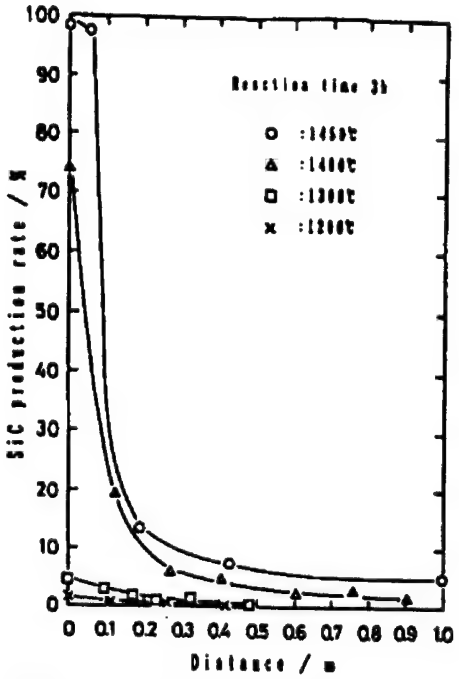

Figure 1. SiC Gradient of SiC/C Materials

Fracture Behavior, Properties of SiC Whisker/Si_3N_4 Composite Ceramics

926C0095K Tokyo NIPPON SERAMIKKUSU KYOKAI 1992 NENKAI KOEN YOKOSHU in Japanese 20 May 92 p 375

[Article by Takayuki Fukawasa, Yasuhiro Goto, and Akihiko Tsuge, Research and Development Center, Toshiba Corp.]

[Text] **Abstract**: The fracture deformation was measured precisely, using SiC whisker/Si_3N_4 composites sintered at various temperatures, and fracture energy (γ_{eff}) was evaluated. As the results, it was recognized that the γ_{eff} was affected by sintering temperature, and the composites had a higher γ_{eff} than monolithic Si_3N_4, particularly for materials sintered at high temperatures. The effect of whisker reinforcement was discussed, and it was noticed that the whiskers work on restraining a catastrophic failure and increasing the fracture energy rather than improving the film thickness K_{IC}.

1. Introduction

In developing structural ceramics, it is an important task to understand their fractural properties in order to improve their strength and film thickness and design reliable materials. In this study, the deformation behavior of SiC whisker reinforced Si_3N_4 composite ceramics was accurately measured and the materials were evaluated from a viewpoint of energy.

2. Experimental Method

The Si_3N_4 and 20 wt% SiC whisker Si_3N_4 composites were hot pressed for sintering at a temperature range at 550~1,770°C. As a sintering assistant, 5wt% Y_2O_3 + 5wt% $MgAl_2O_4$ was used. To stabilize crack development, Chevron notch test slices were used and micro displacements were measured using a differential transformer and the fracture energy was evaluated.

3. Results and Analysis

Figure 1 shows the results of typical load-displacement curves at various sintering temperatures. As the sintering temperature rose, the displacement nonlinearity became greater and changed to a stable fracture behavior. In whisker composite materials, several load fluctuations were observed indicating an existence of the resistivity (rising R-curve behavior) against crack development.

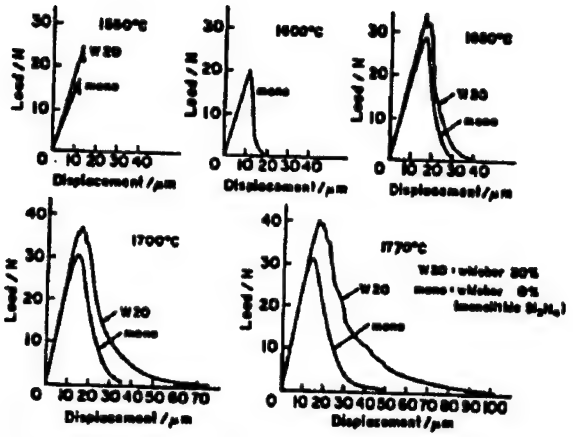

Figure 1. Typical Load-Displacement Curves of Materials Sintered at Various Temperatures

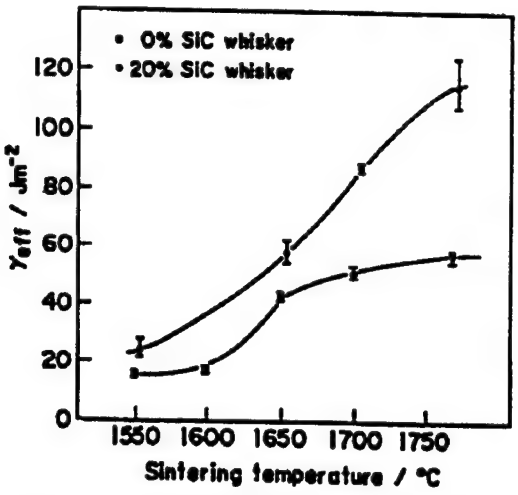

Figure 2. Relationship Between Sintering Temperature and Fracture Energy γ_{eff}

Further, from these results, the fracture energy γ_{eff} was calculated as shown in Figure 2. As the sintering method rose, the effect of adding whisker composites became more conspicuous and a material sintered at 1,770°C in particular needed a fracture energy about double the Si_3N_4 single material, clarifying for the first time the effect of whisker composites of high-temperature sintered materials which had not been detected in the past. It is known that whiskers serve to repress a fracture development and increase the fracture energy. This study was carried out as part of the "elemental technology development of ceramic turbines for coal gasification" consigned to the Fine Ceramic Technology Study Union by the New Energy Industrial Technology Integrated Development Institute based on the next-generation industrial infrastructure technology development system of the Industrial Technology Agency, MITI.

Microstructure, Fracture Toughness of Si_3N_4 Ceramics

926C0095L Tokyo NIPPON SERAMIKKUSU KYOKAI 1992 NENKAI KOEN YOKOSHU in Japanese 20 May 92 p 376

[Article by Takaaki Nagaoka, Koji Watari, Masayoshi Yasuoka, Kiyoji Hirao, and Shuzo Kanzaki, Laboratory, Nagoya Institute of Technology]

[Text] **Abstract:** Three and two-dimensional grain-size distributions of Si_3N_4 ceramics with various microstructures were investigated in order to clarify the relationships between the film thickness and microstructures. It is suggested that there is a correlation between the film thickness and microstructures such as area fraction of large Si_3N_4 grains.

Introduction

In order to upgrade the film thickness of silicon nitride (Si_3N_4) ceramics, the microstructure control measure has attracted attention. Such a control measure is needed to study how to quantify the composition. We[1] previously studied the actual grain-size distribution (three-dimensional distribution) of a Si_3N_4 sintered body prepared by controlling calcination conditions through etching decomposition and taking out each of the Si_3N_4 particles only and compared it with the distribution acquired from the two-dimensional cross section (two-dimensional distribution) and that of K_{IC}. From this study, we clarified that an increase in the volume of fraction of a specific particle group is related to an improvement of K_{IC} and it is necessary to increase the number of measuring samples in order to upgrade the accuracy through acquiring the area of particles, which is the projection of this specific particle group on a two-dimensional distribution.

This time, we calculated the three-dimensional and two-dimensional distributions of Si_3N_4 sintered body prepared by controlling calcination conditions so that larger particles are able to grow easily and further examined the quantitative organization process and examined an organization specifically contributing to the improvement of K_{IC}.

Experiment

The sintered body used for our measurement is an Si_3N_4 (5wt% Al_2O_3-2wt% Y_2O_3) calcined under conditions of Table 1 (E-10) by the Kosan. The relative density

Table 1. Sintering Condition, Relative Density, and K_{IC} of Each Sample

	Sintering condition	Relative density (%)	K_{IC}
A	1	99.1	10.3
B	2	99.1	9.7
C	2	97.8	9.3
D	3	98.2	7.2

1. 1,850°C–4h (45 MPa) → 1,850°C–1h (170 MPa)
2. 1,800°C–4h (40 MPa) → 1,800°C–1h (170 MPa)
3. 1,750°C–4h (40 MPa) → 1,750°C–1h (170 MPa)

of each sintered sample and K_{IC} measured by the single-edge precracked beam (SEPB) are also shown in Table 1.

The three-dimensional or two-dimensional distribution was acquired for scanning electron microscope (SEM) observation after an etching decomposition or polishing etching of samples. The number of samples measured was about 1,500~14,000 for the two-dimensional distribution.

Results

Figure 1 shows an SEM micrograph of the polished and etched surfaces of each sintered sample. Table 2 shows an improvement of K_{IC} and average grain diameter, number fraction compared to all grains, and area fraction as read directly from this SEM micrograph. It is known that the improvement of K_{IC} is closely related to the increase of average grain diameter, number fraction, and area fraction. By acquiring the three-dimensional distribution of these sintered samples, a comparison will be made with the two-dimensional distribution.

Figure 1. Polished and Etched Surface of Sintered Si_3N_4: at 1,850°C

Table 2. Average Grain Diameter, Number Fraction, and Area Fraction of Each Sample

	d_t (μm)	N_f (%)	A_f (%)
A	2.0	33	90.2
B	1.6	9.8	60.2
C	1.5	10.9	49.8
D	1.2	1.1	9.7

$D_t \geq 1$ μm

References

1. Excerpts from Tokai Branch Symposium of Nippon Ceramics Association, 1991, pp 15–16.

Tensile Test of Carbon Fiber-Reinforced Silicon Nitride Sintered Materials

926C0095M Tokyo NIPPON SERAMIKKUSU KYOKAI 1992 NENKAI KOEN YOKOSHU in Japanese 20 May 92 p 378

[Article by Toshihiko Nishida and Ryuichi Saito, Kyoto Institute of Technology, and Misao Iwata, Noritake Co., Ltd.]

[Text] **Abstract:** Effective fracture energies (γ_{eff}) of a carbon fiber-reinforced silicon nitride specimen with circumferential notch were measured by the tensile test. Long pull-out fibers were observed on the fracture surface and also the γ_{eff} values were 3.5 times larger than the values by bending test.

Purpose

Silicon nitride sintered materials reinforced with carbon fibers show a very complicated fracture behavior. As a parameter to represent the "fracture resistivity" of this kind of material, an evaluation of the effective fracture energy (γ_{eff}) is now reviewed.[1] We evaluated the γ_{eff} so far mainly on the flexural test,[2] and it is known from the process of this study that roughly three fracture behaviors would fracture the materials in testing carbon fiber-reinforced ceramics. They are fractures of buckling, delamination, and flexural-isolation-type on flexural faces. As it is hard to isolate these fracture mechanism clearly in the flexural test, we conducted a simplified tensile test this time by observing the fracture behaviors, calculated the γ_{eff} and analyzed a few details.

The sample used was a carbon fiber-reinforced silicon nitride made by Noritake Co., Ltd. With the longitudinal orientation of this fiber as the lengthwise direction, a specimen of the shape (3 x 4 x 40 mm) based on JIS-R1601 was cut out. At the center of this specimen, notches were made from the four sides using a diamond cutter of 0.2 mm thick and a sample of much less area (0.28~1.8 mm^2) was tested for its fracture strength by pulling the two metallic jibs adhered at its both ends in a pin-group method (0.5 mm/minute).

Results and analysis

Figure 1 shows a typical tensile fracture behavior. First, the matrix and fiber were fractured and then a pulling-out of the fiber followed. Though

there were a lot of variations, the γ_{eff} calculated from the relationship of load and displacement was almost consistent without depending on the sample area and its average value was 75 kJ/m^2. This value is about 3.5 times higher than that of the flexural test[2] and a feature was observed that the pulled-out length of carbon fiber remaining on the fracture face was quite long.

This study was conducted as an activity of the Fracture Energy Standardization Subcommittee of the Nippon Ceramics Association.

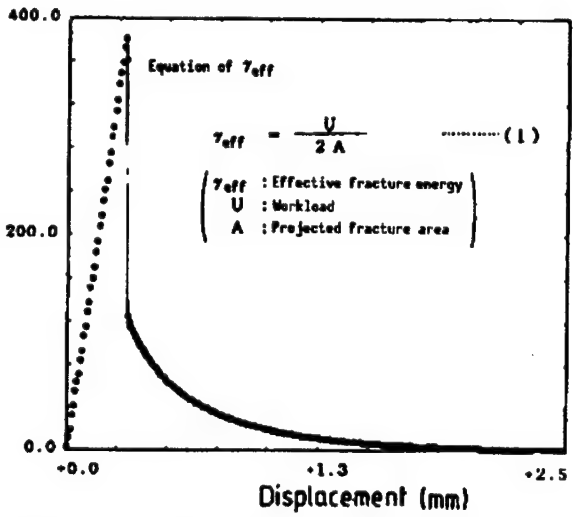

Figure 1. Typical P–u Relation of Tensile Test

References

1. Akatu, T., et al., Proc. 1st Inter. Sympo. Sci. Eng. Ceram., 1991, p 473.

2. Nishida, T., et al., Proc. 34th Japan Congr. Mater. Res., 1991, p 157.

High-Speed Impact Test of Carbon Fiber-Reinforced Silicon Nitride Ceramics

926C0095N Tokyo NIPPON SERAMIKKUSU KYOKAI 1992 NENKAI KOEN YOKOSHU in Japanese 20 May 92 p 379

[Article by Kinya Ogawa, Kyoto University; Toshihiko Nishida, Ryuichi Saito, Kyoto Institute of Technology; and Misao Iwata, Noritake Co., Ltd.]

[Text] **Abstract**: Impact three-point bending tests of a carbon fiber-reinforced silicon nitride were carried out by using a split Hopkinson pressure bar method. Smooth transmitted stress waves without high frequency oscillations were obtained by applying ramped incident waves and were available to evaluate stress-strain relations precisely. γ_{eff} values of the composite were also clarified in the high strain rate range.

Purpose

It is known that there is a considerable variation in the fracture energy of carbon fiber-reinforced silicon nitride ceramics depending on the measurement method, but it is possible to measure it with a better repeatability by the Charpy or Isot impact test.[1] In our study, we aimed at measuring the load-displacement relationship of the flexural impact fracture in a high-speed range of about 10 m/s using the Hopkinson bar method, a highly reliable test method for clarifying impact fracture behaviors.

Experiment

The material used was a carbon fiber-reinforced silicon nitride manufactured by Noritake Co., Ltd. A square rod sample based on JIS-R1601 was used for the specimen (SENB specimen) with a straight notch in the former by an 0.2-mm thick diamond cutter, which was used for the impact fracture test. The specimen was cut with a rectangular notch on its outer edge and the inner edge was ground in parallel, then it was set in an output tube having the fulcrum point between a distance of 30 mm. Then, while arranging one end of the input tube as a knife-edge type pressure point, the specimen was fractured by striking the other end of the tube with a bar through acceleration of compressed air. At that time, a zinc plate was inserted between the bar and the input tube so that ramped incident waves with a gradual rising slope instead of rectangular incident stress waves could be applied.[2]

Results

Figure 1 shows an example of the acquired load-displacement relationship. The maximum load showed a rise of about 20~30 percent in comparison with that of a static flexural test. The γ_{eff} value acquired from these tests was 50~60 kJ/m^2 in a range of (a/W = 0~0.5) without relating to a depth of the notch and the repeatability was quite satisfactory. Furthermore, the data from distortion gauges attached to several spots of the specimen suggested that the fracture of a specimen without notches has transferred from the compressed side (load point) to the flexural face side.

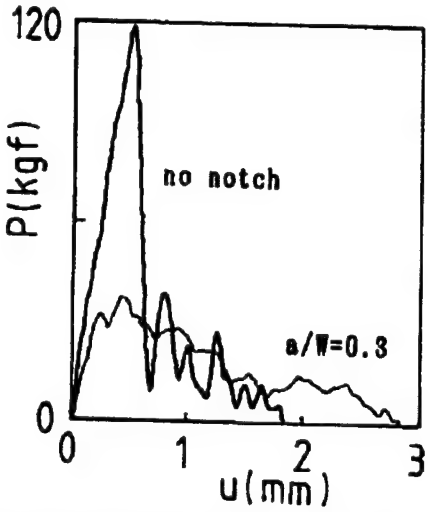

Figure 1. Impact P-u Relationship of CRC

References

1. Akatu, T., et al., Proc. 1st Inter. Sympo. Sci. Eng. Ceram., 1991, p 473.

2. Higashida, F. and Ogawa, K., MATERIALS, Vol 39, 1991, p 1462.

Low Cost β-Silicon Nitride Ceramics

926C00950 Tokyo NIPPON SERAMIKKUSU KYOKAI 1992 NENKAI KOEN YOKOSHU in Japanese 20 May 92 p 380

[Article by Naonobu Hirosaki, Motohide Ando, and Yoshio Akimune, Nissan Motor Co., Ltd., and Mamoru Mitomo, National Institute for Research of Inorganic Materials]

[Text] **Abstract:** Silicon nitride ceramics with a rod-like microstructure were obtained using β-Si_3N_4 raw powder by the grain growth of β-Si_3N_4. These materials are featured to have high reliability, high fracture toughness, and high strength. Low-cost powders can be used in this method.

1. Introduction

It has been said that β-Si_3N_4 powder is not suitable as a raw material as its rod-like structure does not grow in sintering. However, it is possible to have a structure with rod-like crystals grown from micro β-Si_3N_4 particles when they are sintered at high temperature in a gas-pressure sintering method.[1]

When α-powder is used as the raw material, the nuclei of grown grains are the β-type particles with their phases transferred at the early stage and it is hard to control its microstructure as the rod-like growth accompanies the phase transfer. In the meantime, the β-powder generates rod-like crystals with good repeatability to realize various microstructures as large grains in its raw material serve to be the nuclei for grain growth.

Furthermore, low-cost powders of a fireproof grade could be used as the β-type raw material. Therefore, in this study, we developed various materials with the β-Si_3N_4 grain growth technology using the β-Si_3N_4 powder as the starting raw material.

2. Experimental Method

The β-Si_3N_4 powder (A) of sintering grade (high purity, micro powder) and the β-Si_3N_4 powder (B) of fireproof grade (low purity, rough powder) with Y_2O_3-Nd_2O_3 added as the sintering assistant were fabricated into a molding of 6 x 6 x 50 mm after a ball mill blending for the gas-pressure sintering.

After the sintering body was fabricated to 3 x 4 x 40 mm, strength measurement by a three-point bending test was carried out together by the single-edge precracked beam (SEPB) fracture toughness measurement and fractured structure face observation by scanning electron microscope (SEM).

3. Results and Analysis

Reliable material: By growing a structure (self-composite ceramic) including rod-like crystals of several ten μm long using the powder (A), a sintered body with three-point strength of 689 MPa, Weibull coefficient of 53, and fracture toughness of 8.5 $MPam^{1/2}$ was acquired. Making the maximum length of rod-like crystals uniform and distributing them evenly, the variation of strength was minimized and reliability increased.

Strong material: By keeping the growth of rod-like crystals less than 10 μm using the powder (A), a sintered body of three-point bending strength of 984 MPa, Weibull coefficient of 12, and fracture toughness of 5.4 $MPam^{1/2}$ was realized. The strength was enhanced by its microstructure.

Low-cost material: By realizing a structure well grown with rod-like crystals using the powder (B), a sintered body of three-point bending strength of 600 MPa, Weibull coefficient of 11, and fracture toughness of 5.3 $MPam^{1/2}$ was acquired.

Applications of structural ceramics are expected to make progress when low-cost ceramics materials of medium strength, using powders which cost one-fifth to one-tenth the conventional powders, become available.

References

1. Proceedings of the 30th Ceramics Basic Science Symposium, 1992, p 139.

Cyclic Fatigue Properties of Silicon Nitride at High Temperature

926C0095P Tokyo NIPPON SERAMIKKUSU KYOKAI 1992 NENKAI KOEN YOKOSHU in Japanese 20 May 92 p 382

[Article by Takahiro Nishikawa, Hiroshi Katagiri, and Manabu Takatsu, Nagoya Institute of Technology]

[Text] **Abstract**: In this study the authors have carried out cyclic fatigue tests for gas-pressure sintered silicon nitride and sintered silicon nitride of high temperature. The cyclic fatigue properties were estimated by the method using an empirical equation for slow crack growth, and were quantitatively discussed by fatigue parameters (n, log ΔA). The resultant retardative effects of the accelerative effects were observed under cyclic loading. Furthermore, fatigue parameter n depended on temperature.

1. Introduction

In this study, we conducted an experiment on cyclic fatigue properties in a range of temperatures which could be analyzed from the empirical equation of slow crack growth ($V = A(K_I/K_{IC})^n$), using two silicon nitride ceramics with different sintering methods. Further, by using the fatigue parameters (n, log ΔA), the effects of experimental conditions exerted on the cyclic fatigue properties were examined.

2. Experimental Method

For the specimens, silicon nitride samples sintered with gas and normal pressures were used.

For the experimental instrument, a piezo Biemolf-type cyclic fatigue testing unit was used and the required high temperature was acquired by heating the jig section with an electric furnace. Figure 1 shows a photo of the experimental instrument. The cyclic fatigue experiment was conducted under the following conditions: frequency sine wave of 130 Hz and load stress ratio R ($\sigma_{min}/\sigma_{max}$) of a single swing at 1.0, 0.7, and 0.1. The experimental temperature was 300, 450, and 600°C, respectively.

3. Results and Analysis

By introducing the fatigue parameters (n, log ΔA), the cyclic fatigue properties at each temperature were evaluated and the results were summarized in the following.

3.1 Effects of the Load/Stress Ratio

When the log ΔA shows a positive value, it means a faster acceleration effect than a static fatigue of the crack propagation speed in a cyclic load, with a negative value meaning the opposite slower effect. At each experimental temperature, the gas-pressure-sintered silicon nitride sample showed a delayed effect with R = 0.7. Meanwhile, the normal-pressure-sintered silicon nitride sample showed an accelerated effect with R = 0.1.

It is possible that the cause of these effects is that there is indentation damage or wedge effect which increases the crack propagation behavior change and K_I at the crack tip due to different microstructures.

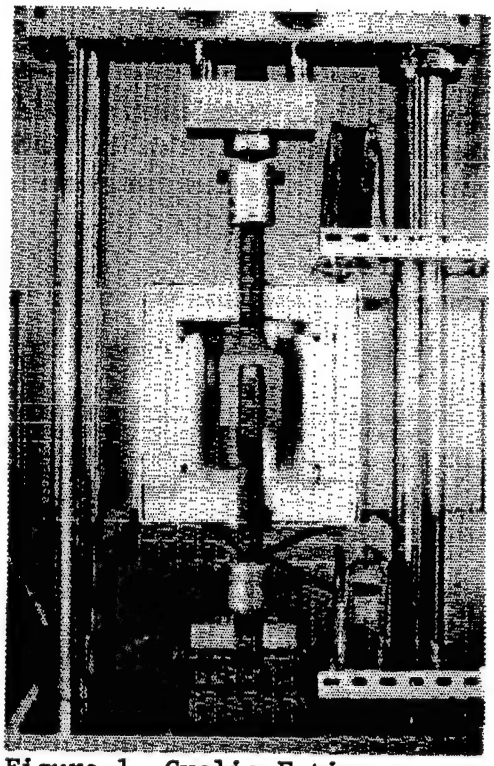

Figure 1. Cyclic Fatigue Testing Instrument for High Temperature

3.2 Effects of Experimental Temperature

The smaller the n value, the larger dependence on the fatigue experiment σ_{max}. With either silicon nitride samples, the n value decreased as the experiment temperature rose. Further, the above-mentioned slow and accelerated effects became inconspicuous at 600°C, partly because of a drop in elasticity at higher temperature.

Atmospheric Effects on Strength of Silicon Nitride, Silicon Nitride Ceramics

926C0095Q Tokyo NIPPON SERAMIKKUSU KYOKAI 1992 NENKAI KOEN YOKOSHU in Japanese 20 May 92 p 383

[Article by Hideyoshi Tsuruta and Yu Furuse, Tokyo Electric Power Co., Ltd.]

[Text] **Abstract**: Four-point bending tests have been carried out at 1,400°C in several atmosphere to examine the effect of atmosphere on strength for silicon carbide and silicon nitride. Strength in vacuum was somewhat lower than those in air, Ar, and N_2 for both materials.

Introduction

When ceramics are used for the gas turbine of 1,500°C class at the turbine inlet, the maximum temperature of its parts may be over 1,600°C. Therefore, it is necessary to be able to evaluate materials at 1,600°C or higher. However, it is difficult to conduct conventional atmospheric strength evaluation because of oxidation problems with jigs, etc. This fact necessitates testing the strength in a nonoxidation atmosphere, but few reports have been made on the effects of the atmosphere under which the strength of ceramics is tested at high temperature. In our study, we measured the strength of silicon nitride and silicon carbide ceramics in the air, argon, nitrogen, and vacuum at 1,400°C. The test was carried out with the cross head speed of 0.5 mm/minute and four-point bending.

Results and Analysis

The strength dependency on atmosphere at 1,400°C is shown in Table 1. Both silicon nitride and silicon carbide samples showed an apparent low strength in vacuum compared with that of other atmospheres but similar values in the air, argon, and nitrogen. When the surface of specimens were observed with an optical microscope, the surface roughness remained almost unchanged in argon and nitrogen before and after the test but a noticeable roughness was observed on the surface in vacuum. One of the reasons for the lower strength in vacuum may be its notable change of roughness on the surface. Therefore, it is desirable to test the strength at high temperature in argon or nitrogen atmosphere. We intend to continue the strength measurement up to 1,600°C in an atmosphere of argon and announce its results at the forthcoming annual meeting.

Table 1. Strength at 1,400°C in Several Atmosphere (MPa)

	In air	In Ar	In N_2	In vacuum
Silicon carbide	520	530	550	430
Silicon nitride	660	615	620	560

Controlling Microstructure of Si_3N_4 Ceramics With Y_2O_3, Al_2O_3 Additives

926C0095R Tokyo NIPPON SERAMIKKUSU KYOKAI 1992 NENKAI KOEN YOKOSHU in Japanese 20 May 92 p 384

[Article by Katsutoshi Komeya, Yokohama National University/Kanagawa Science and Technology Academy, and Yasushi Haruna and Takeshi Meguro, Yokohama National University]

[Text] **Abstract:** Microstructural development of Si_3N_4 with Y_2O_3 and Al_2O_3, was widely investigated by the selection of raw powders, compositions, and firing profiles. It becomes evident that elongation and grain growth markedly appears with increasing Y_2O_3/Al_2O_3 which is affected by the properties of raw powder characteristics. Fracture toughness was dependent on composition and firing conditions. It is presumed that large and elongated grain structure brings higher fracture toughness.

1. Purpose

For Si_3N_4–Y_2O_3–Al_2O_3–based sintered ceramics, the relationship of their microstructural change, fracture toughness, and microstructures dependent on their raw material powders, compositions, and sintering conditions were examined.

2. Experiment

After wet blending in a ball mill specified quantities of three Si_3N_4 powders of different preparing methods (imide decomposition (A), reducing nitridation (B), and direct nitridation (C)), Y_2O_3 and Al_2O_3, the blend was molded, degreased, and its step-1 calcination was conducted by gas-pressure sintering and the step-2 calcination by hot pressing. After sintering, each specimen was measured for its density, X-ray diffraction, scanning electron microscope (SEM), transmission electron microscope (TEM), and fracture toughness test (IF method). Here, the composition added with 5 wt%Y_2O_3–2 wt%Al_2O_3 is expressed as 5Y2A and similarly 2Y5A and 5Y5A are used.

3. Results and Analysis

Figure 1 shows SEM micrographs of fractured surfaces of specimens after sintering the powder (A) for six hours at 1,800°C. No growth of rod-like

Figure 1. SEM Photographs of Fractured Surfaces of Step 1-Sintered Specimens for A Powder (1,800°C, 6 hours)

particles is observed without Y_2O_3 additives but Y_2O_3-added specimen changed its particular shape greatly by a ratio of Y_2O_3/Al_2O_3 and it was observed that the greater the ratio the more prominent the particle growth and rod-like growth. By changing the additive quantity of sintering assistants in this way, it has been confirmed that it is possible to control crystalline grain shapes in the sintering structure. Further, we analyzed the behavior of grain growth by comparing microstructures of sintered specimens manufactured from each raw material powder. When powder (B), with large granularity distribution, was used, the grain growth became prominent and, as a result, its density process was hampered.

Figure 2 shows a relationship between the fracture toughness value and composition ratio of powder (B) with different step-1 calcination temperature. Different values of the fracture toughness were obtained by varying the composition and calcination conditions. These results can be explained that the generation and growth of rod-like particles and existence of grain boundary phase raises the resistivity of crack propagation. From the above, it is confirmed that high fraction toughness values can be realized when the grain growth is quick and the aspect ratio of rod-like grains is large. In the case of step-1 calcination at 1,850°C in Figure 2, the 5Y5A shows a higher fraction toughness than 5Y2A, but this difference may be attributed to a combination of the aspect ratio and crystalline grains getting rougher.

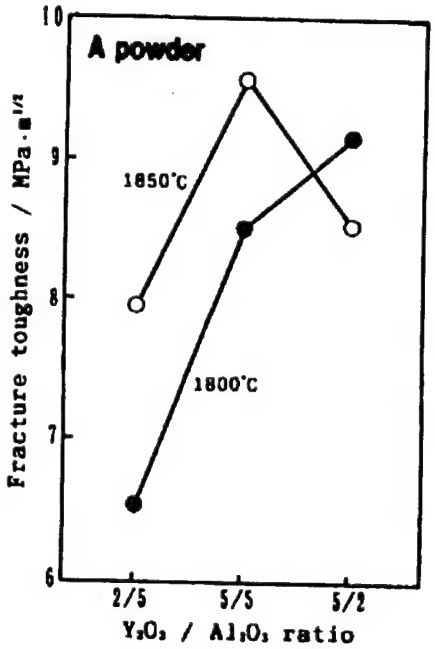

Figure 2. Fracture Toughness of Step 2-Sintered Specimens

Direct Bonding of Ceramics by Metallization Through Ion Beam Dynamic Mixing

926C0095S Tokyo NIPPON SERAMIKKUSU KYOKAI 1992 NENKAI KOEN YOKOSHU in Japanese 20 May 92 p 395

[Article by Nakaya Chida, Masamichi Matsuura, Y. Wang, and Sonoko Tsukahara, Institute of Super Materials, ULVAC Japan, Ltd.]

[Text] **Abstract**: Cu or Ni metallization of Si_3N_4, SiC, and Al_2O_3 substrates was performed using an ion beam dynamic mixing. In this method, an energetic Ti^+ ion beam and a metal vapor (Cu, Ni) were irradiated simultaneously onto a ceramic to deposit a metal film. A metallized ceramic was directly bonded to a Cu or Ni rod under vacuum at 573~773 K, resulting in a strong joint of >80 MPa for each type of ceramics.

1. Introduction

The dynamic mixing method is a means to irradiate high-energy ions and conduct a metallic vapor-deposition simultaneously on the substrate, featuring a capability of forming a highly adhesive film on the substrate. We conducted Mo-metallization onto Al_2O_3, SiC, and Si_3N_4 structural ceramics using this method and further brazed them to a bulk Cu.

We previously reported[1] that it is possible to have a joint body of ceramics and Cu having a tensile strength of 120~160 MPa. This time, we tried to bond the metallized film and metal directly in a solid-phase bonding without using a blazing agent, subsequent to the former report on bonding ceramics and metal using the dynamic mixing method.

2. Experiment and Results

The Al_2O_3, SiC, and Si_3N_4 substrates are ϕ5 x 15 sintered materials (Kyocera: A-479, SN-220, SC-211) with their end faces mirror-ground. Ti^+ ion for the dynamic mixing and Cu and Ni for the simultaneous vapor deposition were selected and a metallized film of about 5 μm thick was acquired under the conditions (ion radiation: ion energy -50 KeV, ion current density 10 $\mu m/cm^2$, metallic vapor deposition: vapor-deposition speed 0.1~1.0 nm/s, substrate temperature: 573 K) almost similar to the last experiment. The metallized substrate was supplied to the solid-phase bonding in vacuum after aerating it once. The bonding was done in a combination of a metallized film and a similar

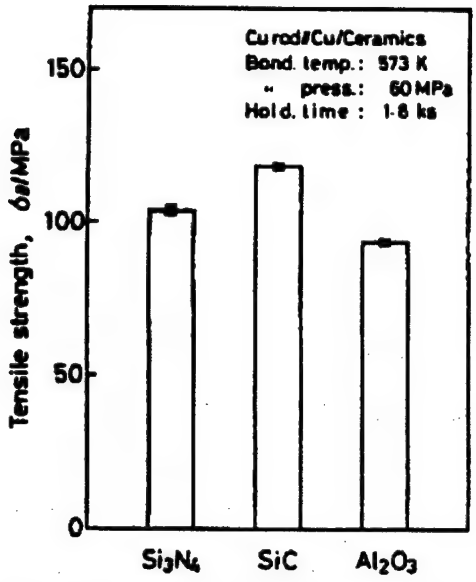

Figure 1. Tensile Strength of Directly Bonded Cu/Ceramics Joints Using Cu Metallization

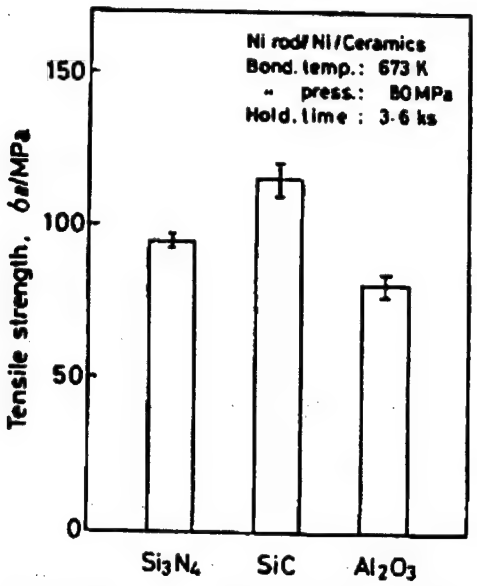

Figure 2. Tensile Strength of Directly Bonded Ni/Ceramics Joints Using Ni Metallization

metallic rod under the conditions of temperature at 523~723 K and atmospheric pressure of 60~120 MPa. Sputter cleaning was applied to the bonded face in advance by means of a glow discharge in the Ar–H_2 atmosphere.

Examples of the acquired results are shown in Figures 1 and 2. The ceramics/Cu/bulk Cu and ceramics/Ni/bulk Ni specimens of Al_2O_3, SiC, and Si_3N_4 ceramics each realized bonded materials having a tensile strength of 80~120 MPa.

References

1. Chida, Fujinuma, Matsuura, and Tsukahara, Nippon Ceramics Association, 1991 Annual Seminar Proceedings, 1A 08, p 8.

Oxidation Behavior of Silicon Nitride, Sialon Ceramics

926C0095T Tokyo NIPPON SERAMIKKUSU KYOKAI 1992 NENKAI KOEN YOKOSHU in Japanese 20 May 92 p 396

[Article by Katsutoshi Komeya, Yokohama National University/Kanagawa Science and Technology Academy; Kazuo Funabashi, Takeshi Meguro, Yokohama National University; Tsuneharu Kameda, Masahiro Asayama, Toshiba Corp.; and Shoki Umebayashi, GIRIK]

[Text] **Abstract:** Si_3N_4 specimen was prepared from Si_3N_4–Y_2O_3–Al_2O_3 system, and $Si_{6-Z}Al_ZO_ZN_{8-Z}$ (Z = 0.5) was used as a Sialon. Oxidation of specimens was conducted under the condition of in dry and wet air flow at 1,100~1,400°C. It was confirmed that the oxidation was drastically affected by the starting compositions and the existence of water vapor in oxidizing atmosphere.

1. Purpose

We aimed at clarifying the oxidation behavior by oxidizing silicon nitride and sialon sintered specimens and, in particular, at examining the effect of oxidation due to a difference of their composition.

2. Experiment

As the silicon nitride specimen, a β–Si_3N_4 sintered body with Y_2O_3, Al_2O_3, and AlN additives in an α–Si_3N_4 powder was used. Meanwhile, a β–sialon ($Si_{6-Z}Al_ZO_ZN_{8-Z}$) with Z = 5 was used. From these sintered bodies, sample slices (3 x 4 x 20 mm) were cut out and oxidized at 1,100~1,400°C in a dry and wet air flow (2.3 vol H_2O%) for our analytical comparison.

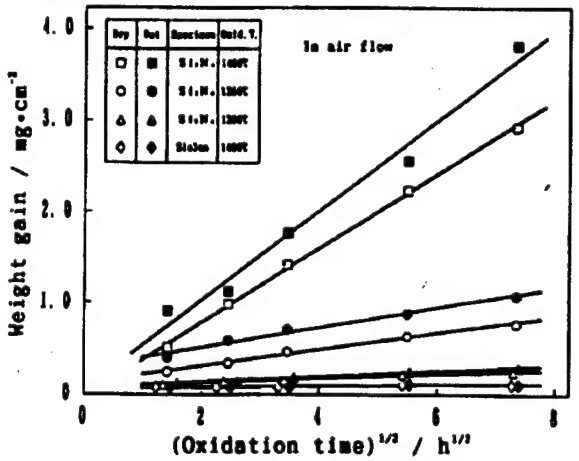

Figure 1. Parabolic Plots for Oxidation of Si_3N_4 and Sialon Specimens

3. Results and Analysis

Figure 1 shows a relationship between the weight increase by oxidation and (oxidizing time)$^{1/2}$. Except for the initial reaction, its linearity is

satisfactory and it is recognized that this reaction is following a diffusion controlled parabolic plot. The activated energy of silicon nitride specimens was 628 and 616 kJ/mol, respectively, in the dry and wet air. Meanwhile, it was hard for the sialon specimens to calculate their activated energy as the weight increase by oxidation was minimal. As a result of examining the change of crystalline phase accompanying oxidation, it was discovered that the silicon nitride specimen tends to increase its generation of α-cristobalite and $Y_2O_3 \cdot 2SiO_2$ as the oxidation temperature rises, confirming the fact that this increasing trend differs depending on the atmosphere. Meanwhile, the sialon specimen generates only a little of α-cristobalite irrelevant of the oxidation temperature and atmosphere and no other substances were generated.

As a result of observing the surface of specimens after oxidation, it was discovered that the surface of silicon nitride specimen gets roughed at 1,300°C both in a dry and wet atmosphere. In a dry atmosphere at 1,350°C, a similar surface was observed but, in a wet atmosphere, the whole specimen was covered with a glass-like product and large granular crystals were observed underneath. It was also observed that the sialon specimen developed a smooth surface regardless of the atmosphere, and this was confirmed by measuring the surface roughness.

Table 1. SEM Photographs for Oxidized Specimens of Silicon Nitride

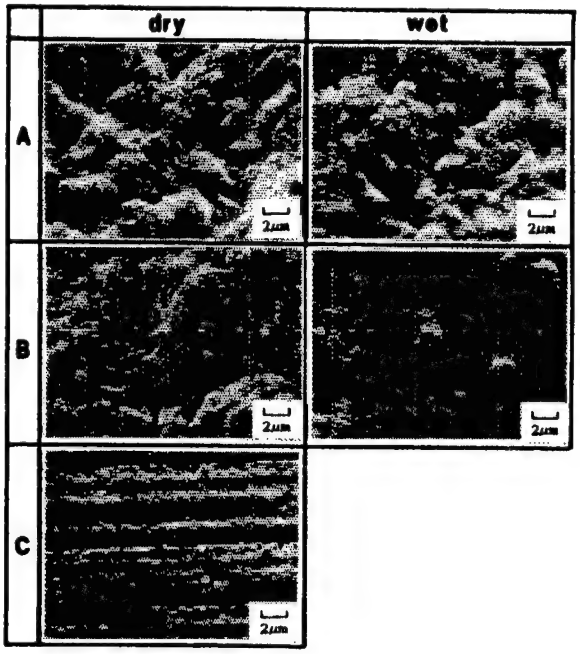

A. 1,300°C
B. 1,350°C
C. Original surface

Corrosion Behavior of Ceramics in High-Temperature Combustion Gas Flow

926C0095U Tokyo NIPPON SERAMIKKUSU KYOKAI 1992 NENKAI KOEN YOKOSHU in Japanese 20 May 92 p 397

[Article by Yasuyuki Endo, Hideyoshi Tsuruta, and Yu Furuse, Tokyo Electric Power Co., Ltd.]

[Text] **Abstract:** Corrosion behavior of ceramics was investigated under operational conditions of gas turbines. Weight loss of the nonoxide specimens was observed after the exposure to high-temperature gas flow under pressurized conditions. The test results for oxide coated specimens showed the possibility of increasing the corrosion resistance of nonoxide ceramics.

1. Introduction

When nonoxide ceramics of silicon nitride and silicon carbide are used for gas turbine components, the materials are exposed to high temperature, speed, and pressure for a long period of time. In a previous study,[1] it was discovered that the material tends to decrease in weight regardless of what kind of material it is when each ceramic sample piece is exposed to combustion gas similar to that of actual turbines at high temperature and for a long time. In our study, we will report on the experiment conducted to estimate the weight-reduction mechanism and testing results of a surface coating conducted to improve the antioxidation and corrosion resistance properties.

2. Experiment

(1) Experimental Equipment

The experiment was carried out by modifying combustion testing equipment for gas turbine and kerosene, methane gas, and LP gas (main element: butane) were used for its fuel). In order to avoid abrasion loss during flight, filters were installed over the fuel and air system pipes. To prevent unburnt carbons from exerting any effect, a perfect combustion system was considered. With this equipment, it is possible to test up to the maximum conditions of 1,500°C, 8.5 ata, and flow speed of 370 m/s.

(2) Test Materials

The materials provided for testing were: 1) Si_3N_4 and SiC specimens sintered under normal pressure which are commercially available as well as under development; 2) the same sintered Si_3N_4 and SiC, but coated with Si_3N_4 and SiC films by the chemical vapor deposition (CVD) method; 3) silicon nitride material coated with oxide ceramics; and 4) oxide ceramics.

3. Results and Analysis

Figure 1 shows a relationship between the temperature/pressure and the weight loss of a silicon nitride specimen after a 10-hour exposure test. It is clear that the weight reduction accelerates as the temperature and pressure are increased. Meanwhile, the flow velocity effect on the weight reduction is not so prominent. These trends are similar in other materials, confirming that usage of different fuels and filters does not matter. From these facts, it is estimated that the weight loss occurred because the glass layer formed on the surface through oxidation was blown away by the high-velocity gas. This poses an intrinsic problem unavoidable under the gas turbine environment.

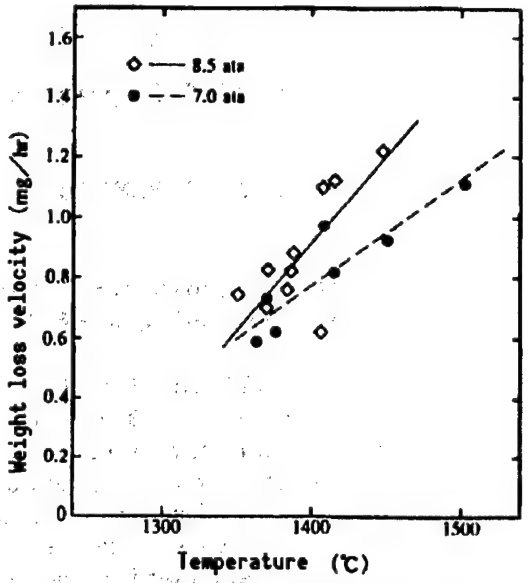

Figure 1. Relationship Between Temperature/Pressure and Weight Loss Velocity of Specimens (Si_3N_4 materials)

As to the specimen with an oxide coating over the surface of silicon nitride material, a minimizing effect of weight loss was observed under the conditions of 1,400°C, 8.5 ata, 300 m/s and 10 hours, indicating the possibility of improving antioxidation and corrosion resistance.

References

1. Furuse, et al., Nippon Ceramics Association Second Autumn Symposium Proceedings, 1989, pp 178-179.

Corrosion Behavior of SiN Ceramics in Water, Saturated Steam at High Temperature

926C0095V Tokyo NIPPON SERAMIKKUSU KYOKAI 1992 NENKAI KOEN YOKOSHU in Japanese 20 May 92 p 398

[Article by Tetsuo Yoshio and Takeshi Suemasu, Okayama University, and Kohei Oda, Yonago National College of Technology]

[Text] **Abstract:** Silicon nitride ceramics were exposed to distilled water and saturated steam at 300°C (8.6 MPa) for periods up to 10 days. Their corrosion behavior was studied and also corrosive strength degradation was estimated. The specific weight loss vs. exposure time obeyed parabolic law for water corrosion and linear law for steam corrosion. Weight loss and thickness of corroded layer for steam corrosion were larger than those for water corrosion. However, strength degradation was similar to the trend for both corrosion. It showed the catastrophic degradation in the early stage of corrosion within one-day exposure. It might come from original surface finishing conditions. This corrosion behavior is approximately the same with the results in our previous work on mullite ceramics.

Introduction

In evaluating the corrosiveness of structural ceramics in water under a high-temperature and high-pressure environment, it is essential to study the corrosion behavior both in water and coexisting saturated steam. In succession to the corrosion behavior reported before for the mullite ceramics in water and coexisting saturated steam at 300°C, this study will discuss a similar evaluation test of silicon nitride ceramics.

Experiment Method

The silicon nitride specimen used is a material sintered at normal pressure fabrication based on JIS-R1601 showing the characteristics given in Table 1. The experiment and corrosion tests were conducted under similar conditions as the mullite ceramics.[1]

Table 1. Characteristics of Si_3N_4

Sintering aids (wt%)	Density (g/cm^3)	Bending strength (MPa)
Y_2O_3:5.00 Al_2O_3:3.76	3.26	912

Results and Analysis

Figure 1 shows the measurement results of corrosion weight loss after exposure to the liquid and vapor phases at 300°C and under 8.6 MPa (equilibrium steam pressure). In the liquid phase, the specimen followed a parabolic law and in the vapor phase a linear law, similar to the corrosion behavior of the mullite ceramics in that the weight loss was more drastic in the vapor phase. Further, it is known that the thickness of a corroded layer is greater and more noticeable in the saturated steam than in the liquid phase though the produced corrosive substances are different. However, the characteristic of SiO_2 composition which contributes to the weight loss in the vapor phase is still unknown while the weight loss in the liquid phase is due to dissolution of SiO_2.

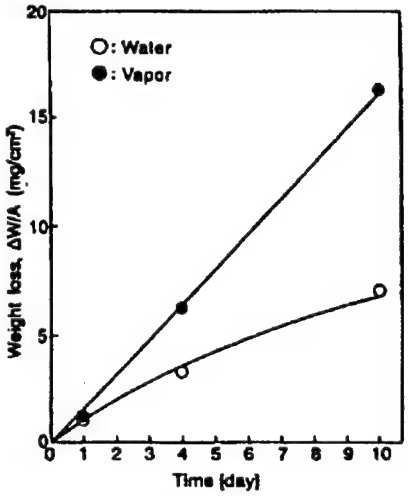

Figure 1. Weight Loss Vs. Exposure Time for Si_3N_4 Exposed to Water and Steam at 300°C

Figure 2 shows the measurement of a three-point bending strength in liquid and vapor phase processing at room temperature. As to the strength degradation trend, a large degradation was first observed after one-day processing and then it became constant just like that of mullite ceramics though a big difference exists in the corrosion weight loss and corrosive layer thickness depending on the liquid or vapor phase processing. Pitting and a trace of grinding at the time of processing are observed on the surface of the base material after removing the corrosive layer which was made within one-day exposure. This seems to translate into rapid strength degradation at the early corrosion stage due to the processing hysteresis of the surface.

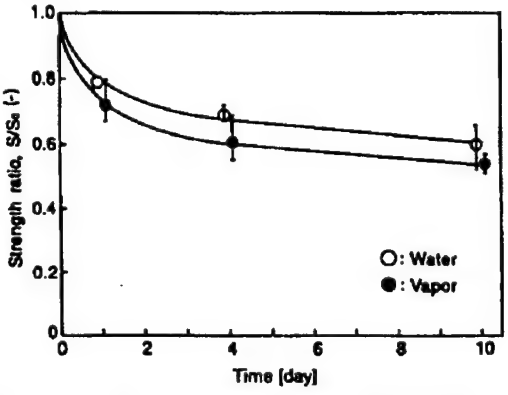

Figure 2. Bending Strength Vs. Exposure Time for Si_3N_4 Corroded in Water and Steam at 300°C

References

1. Sakuta, Suemasu, Yoshio, and Oda: 30th Ceramics Basic Scientific Discussion Seminar Proceedings, 1992, p 64.

Corrosion of SiN, SiC Ceramics in Caustic Alkaline Solutions

926C0095W Tokyo NIPPON SERAMIKKUSU KYOKAI 1992 NENKAI KOEN YOKOSHU in Japanese 20 May 92 p 399

[Article by Tsugio Sato, Shigeki Sato, Kazuhiro Tamura, and Akitsugu Okuwaki, Faculty of Engineering, Tohoku University]

[Text] **Abstract:** Corrosion behaviors of Si_3N_4 and SiC ceramics were investigated in 0~25 m NaOH solutions at 150~300°C. Si_3N_4 ceramics were susceptible to attack in NaOH solutions above 150°C. SiC ceramics were stable in 25 m NaOH solutions up to 300°C in the absence of oxygen, but were susceptible to corrosive attack in the presence of oxygen.

Introduction

It is important to evaluate the chemical stability of ceramic materials as the environment under which they are used is varied and extensive. This study discusses the corrosion behavior of Si_3N_4 and SiC ceramics in an NaOH solution.

Experiment

Specimens of hot-pressed Si_3N_4 (HP-Si_3N_4), and ordinary-pressure sintered Si_3N_4 (S-Si_3N_4), ordinary-pressure sintered α-SiC and β-SiC ceramics were reacted in 0~25 m NaOH water solutions with partial oxygen pressure of 0~5 MPa at 150~300°C for a specified time, and their weight loss, strength degradation and changes of their surface microstructure were examined.

Results and Analysis

(1) Corrosion in Absence of Oxygen

The SiC remained stable in an NaOH solution up to 300°C but the Si_3N_4 ceramics corroded above 150°C and the corrosion resistance was better for the HP-Si_3N_4 ceramics than the S-Si_3N_4 ceramics (Figure 1). The corrosion rate is proportional to the secondary NaOH concentration and the apparent activated energy was 164 kJ/mol. From this, the

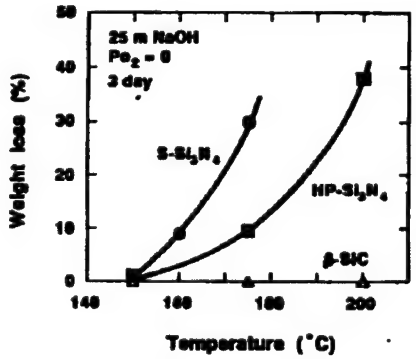

Figure 1. Corrosion Without Oxygen

reaction can be expressed in the following two equations. Equation (2) seems to denote a diffusion law.

$$Si_3N_4 + 6H_2O \rightarrow 3SiO_2 + 4NH_3 \quad (1)$$

$$SiO_2 + 2OH^- \rightarrow SiO_3^{2-} + H_2O \quad (2)$$

As the corrosion progresses, a porous Si_3N_4 layer of 100~300 μm is formed on the specimen surface, and the fracture strength of specimens dropped quickly from 1,000 MPa to 500 MPa while the S-Si_3N_4 specimen reduced its weight by 2 percent and the HP-Si_3N_4 specimen dropped from 1,000 MPa to 150 MPa while its weight decreased by 15 percent, and then they maintained an almost consistent strength.

(2) Corrosion in Presence of Oxygen

The SiC ceramics showed a drastic weight loss under an oxygen pressure and its corrosion rate was almost similar both for α-SiC and β-SiC specimens. The corrosion rate was proportional to the NaOH concentration up to 1 m but decreased above it (Figure 2).

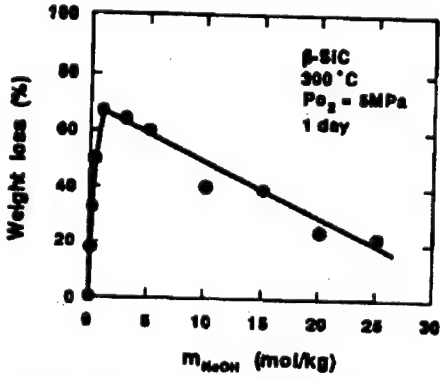

Figure 2. Corrosion With Oxygen

The lowering of the corrosion rate in the highly concentrated NaOH may be attributable to the lowering dissolution of oxygen. Further, the corrosion rate increased proportional to the first partial pressure of oxygen under a low partial pressure of oxygen, but became constant under a high partial pressure of oxygen. From this result, in the corrosion reaction, the absorption of oxygen toward the specimen is diffused in a high NaOH concentration and under low partial pressure of oxygen, and the dissolving process of SiO_2 is diffused in a low NaOH concentration and high oxygen partial pressure. The fracture strength decreases drastically from 500 MPa to 400 MPa at the early reaction stage and then gradually—about 170 MPa—when the weight decreases by 60 percent.

Thermal Shock Resistance of SiC-Whisker Reinforced Si_3N_4 Ceramics

926C0095X Tokyo NIPPON SERAMIKKUSU KYOKAI 1992 NENKAI KOEN YOKOSHU in Japanese 20 May 92 p 550

[Article by Yu Sato and Masanori Ueki, Nippon Steel Corp., and Mitsuo Sugawara, EC Manufacturing Division, Kurosaki Corp.]

1. Introduction

We previously proposed a method[1] of evenly dissipating whiskers, prepared composite materials of different whisker additive quantities with this method, and compared the static fracture toughness value[2] based on JIS-R1607 (single-edge precracked beam (SEPB)-method) with the dynamic fracture toughness value (impact value)[3] based on the Charpy test. It was discovered they have no relative relationship and the impact value depends on the three-point bending strength at room temperature. With the whisker composite materials, in addition to improving toughness, upgrading the thermal shock characteristics is expected by adding SiC whiskers of superior thermal conductivity. In this study, we conducted thermal shock resistance tests by rapidly quenching Si_3N_4 and SiC-whisker reinforced Si_3N_4 materials in water and examined them for comparison.

2. Experimental Method

As the samples of the thermal shock resistance test, normal-pressure sintered body (PLS) of blended powder on the market using a Y_2O_3-Al_2O_3-based auxiliary was used for the Si_3N_4 specimen. For the SiC-whisker reinforced Si_3N_4, the Si_3N_4 matrix powder using a Y_2O_3-Al_2O_3-based auxiliary as well with 20 wt% SiC whiskers added was used. Their plate samples hot pressed (HP) under a pressure of 40 MPa were cut into specimens of 3 x 4 x 40 mm each and tested for a three-point bending strength at room temperature (JIS-R1601). Further, after a rapid quenching test at a range of ΔT 200~1,200°C as a thermal shock test, separate specimens were exposed to a three-point bending strength test as well for comparison of their strength.

3. Results and Analysis

A relationship between the three-point bending strength after quenching the samples and the ΔT is shown in Figure 1. The Si_3N_4 specimen lowered its

strength at 600°C, getting worse at 700°C and dropped its average strength drastically at 750°C. In contrast, the SiC-whisker reinforced Si_3N_4 specimen started its strength change at 1,050°C and some samples showed a strength degradation but did not show a drastic drop as that of the Si_3N_4 specimen up until 1,200°C even though the strength was unstable at high temperature. The thermal conductivity of Si_3N_4 and SiC-whisker specimens was 28.4 and 34.3 kcal/m·h·k, respectively, and it is presumed that the upgrading of thermal conductivity by the SiC whisker reinforcement contributes greatly to improving the thermal shock resistance. Furthermore, the SiC-whisker reinforced Si_3N_4 specimen did not show a drastic drop in strength even with ΔT more than the temperature difference where some samples degraded in strength and it is estimated that the crack generation and its growth due to thermal stress were restrained by the whisker incorporation.

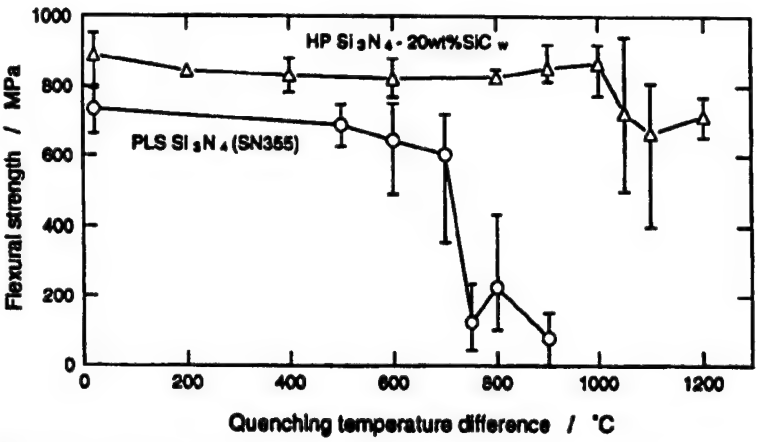

Figure 1. Correlation Between Quenching Temperature and Flexural Strength of Si_3N_4 and Si_3N_4-20wt% SiC_w

References

1. Sato, et al., Nippon Ceramics Association, 1990 Seminar Proceedings, p 92.

2. Ibid., 1991 Seminar Proceedings, p 403.

3. Taira, et al., 1991 Seminar Proceedings, p 409.

Application Results of Plasma Sprayed $2CaO \cdot SiO_2$-$CaO \cdot ZrO_2$ Coatings on Stator Vanes for Gas Turbine

926C0095Y Tokyo NIPPON SERAMIKKUSU KYOKAI 1992 NENKAI KOEN YOKOSHU in Japanese 20 May 92 p 552

[Article by Niroshi Imawaka, Hatsuo Taira, Shin'ichi Tamura, and Yasuaki Shinohara, Technical Development Bureau, Nippon Steel Corp., and Shoji Mishima, Motoyoshi Fukuma, and Kazuya Kuroiwa, Hirohata Works, Nippon Steel Corp.]

[Text] **Abstract:** Stator vanes spray coated with $2CaO \cdot SiO_2$–$CaO \cdot ZrO_2$(C_2S–CZ) system ceramics were operated in actual service for about 13,000 hours. The abrasion of C_2S–CZ coatings was negligibly small. Perpendicular cracks were observed in C_2S–CZ coatings, but the substrate was not damaged.

1. Introduction

In our previous reports,[1,2] we studied the thermal shock resistance and corrosiveness of $2CaO \cdot SiO_2$–$CaO \cdot ZrO_2$ spray coatings. Here, we are going to report our application results of spraying C_2S–15wt%CZ and C_2S–20wt%CZ coatings as well as a representative ZrO_2–8wt%Y_2O_3 coating onto the stator vane of a gas turbine and operating the turbine for about 13,000 hours.

2. Method

After a blast processing of the stator vane in operation, an Ni–alloy bonded layer (about 100 μm thick) and ceramic layer (about 200 μm thick) were sprayed on it. Main application conditions are shown in Table 1. The stator vane was observed and analyzed for its coating cross section using scanning electron microscope–electron probe microanalyzer (SEM–EPMA) after operating the turbine for about 13,000 hours.

3. Results and Analysis

(1) Surface Condition

Extraneous matters increased centering around the concave side of the stator vane. The C_2S–15wt%CZ coating had a chipping of about ϕ5 mm on the convex side

Table 1. Operating Condition

Dynamo capacity	Maximum 30.2 MW
Combustion gas temperature at vanes	1,292 K
Kinds of fuel	LDG, oil
Operation time	13,000 hours
Number of restarts	110 times

Table 2. Comparison of Damage and Residual Thickness of Coatings After Actual Use

Ceramic coating		C_2S–15%CZ		C_2S–20%CZ		ZrO_2–8wt%Y_2O_3	
		Damage	Thick-ness (μm)	Damage	Thick-ness (μm)	Damage	Thick-ness (μm)
Part of the vane	Convex side	SC	200	NC	200	NC	200
	Concave side	NE	200	NE	200	NP	100~200
	Leading edge	NE	200	NE	200	E	50~150

SC: Slight chipping; NC: No chipping; NE: No exfoliation;
EP: Exfoliated partially; E: Exfoliation

but no exfoliation was observed. Meanwhile, the ZrO_2–8wt%Y_2O_3 coating had a partial exfoliation on part of the concave side and leading edge, showing worse damage than the C_2S–CZ coating (Table 2).

(2) Observation of the Cross Section

The C_2S–CZ coating remained at about 200 μm on the leading edge and almost no wear was observed. Further, both of the coatings had cracks reaching the bonded layer but no exfoliation between layers. S and Ca were detected in the piercing cracks of C_2S–15wt%CZ coating and the deposit on its surface included Fe, Ca, Si, Al, and S but no abnormalities near the bonded layer. This is a result of the S component of combustion gas penetrating into the cracks generated in operation and solidifying as $CaSO_4$ reacting with the Ca component of the coating. Meanwhile, the ZrO_2–8wt%Y_2O_3 coating cross section on the concave side of the stator vane had vertical cracks from the surface layer and continuous exfoliation between layers. Further, the leading edge had an exfoliation with the residual coating of about 50 μm in the bonded layer. As described above, it was discovered that the C_2S–CZ-based spray coating using many vertical microcracks in its coating film is superior in resistance.

References

1. Imawaka, H., Taira, H., Kanematsu, K., Tamura, S., Yamane, H., and Harada, Y., Nippon Ceramics Association, 1991 Annual Meeting Proceedings, 3E01.

2. Imawaka, H., Taira, H., Kanematsu, K., Shin-ichi, S., Yogoro, T., and Mifune, N., Same proceedings, 3E32.

- END -

Foreign Broadcast Information Service (FBIS) and Joint Publications Research Service (JPRS) publications contain political, military, economic, environmental, and sociological news, commentary, and other information, as well as scientific and technical data and reports. All information has been obtained from foreign radio and television broadcasts, news agency transmissions, newspapers, books, and periodicals. Items generally are processed from the first or best available sources. It should not be inferred that they have been disseminated only in the medium, in the language, or to the area indicated. Items from foreign language sources are translated; those from English-language sources are transcribed. Except for excluding certain diacritics, FBIS renders personal names and place-names in accordance with the romanization systems approved for U.S. Government publications by the U.S. Board of Geographic Names.

Headlines, editorial reports, and material enclosed in brackets [ ] are supplied by FBIS/JPRS. Processing indicators such as [Text] or [Excerpts] in the first line of each item indicate how the information was processed from the original. Unfamiliar names rendered phonetically are enclosed in parentheses. Words or names preceded by a question mark and enclosed in parentheses were not clear from the original source but have been supplied as appropriate to the context. Other unattributed parenthetical notes within the body of an item originate with the source. Times within items are as given by the source. Passages in boldface or italics are as published.

SUBSCRIPTION/PROCUREMENT INFORMATION

The FBIS DAILY REPORT contains current news and information and is published Monday through Friday in eight volumes: China, East Europe, Central Eurasia, East Asia, Near East & South Asia, Sub-Saharan Africa, Latin America, and West Europe. Supplements to the DAILY REPORTs may also be available periodically and will be distributed to regular DAILY REPORT subscribers. JPRS publications, which include approximately 50 regional, worldwide, and topical reports, generally contain less time-sensitive information and are published periodically.

Current DAILY REPORTs and JPRS publications are listed in *Government Reports Announcements* issued semimonthly by the National Technical Information Service (NTIS), 5285 Port Royal Road, Springfield, Virginia 22161 and the *Monthly Catalog of U.S. Government Publications* issued by the Superintendent of Documents, U.S. Government Printing Office, Washington, D.C. 20402.

The public may subscribe to either hardcover or microfiche versions of the DAILY REPORTs and JPRS publications through NTIS at the above address or by calling (703) 487-4630. Subscription rates will be provided by NTIS upon request. Subscriptions are available outside the United States from NTIS or appointed foreign dealers. New subscribers should expect a 30-day delay in receipt of the first issue.

U.S. Government offices may obtain subscriptions to the DAILY REPORTs or JPRS publications (hardcover or microfiche) at no charge through their sponsoring organizations. For additional information or assistance, call FBIS, (202) 338-6735,or write to P.O. Box 2604, Washington, D.C. 20013. Department of Defense consumers are required to submit requests through appropriate command validation channels to DIA, RTS-2C, Washington, D.C. 20301. (Telephone: (202) 373-3771, Autovon: 243-3771.)

Back issues or single copies of the DAILY REPORTs and JPRS publications are not available. Both the DAILY REPORTs and the JPRS publications are on file for public reference at the Library of Congress and at many Federal Depository Libraries. Reference copies may also be seen at many public and university libraries throughout the United States.